Systematically Convergent Correlation Consistent Basis Sets for Molecular Core−Valence Correlation Effects: The Third-Row Atoms Gallium through Krypton†

Nathan J. DeYonker,*,‡ Kirk A. Peterson,§,# and Angela K. Wilson‡,£

Center for Advanced Scientific Computing and Modeling (CASCaM), Department of Chemistry, University of North Texas, Denton, Texas 76203, and Department of Chemistry, Washington State University, Pullman, Washington 99164

Received: June 19, 2007; In Final Form: September 4, 2007

The family of correlation consistent polarized valence basis sets has been extended in order to account for core−core and core−valence correlation effects within the third-row, main group atoms gallium through krypton. Construction of the basis sets is similar to that of the atoms boron through argon, where either the difference between core-correlated and valence-only correlation energies were calculated via configuration interaction (CISD) computations on the ground electronic states of the atoms (named cc-pCV*n*Z) or the sets were optimized with respect to the core−valence correlation energy and a small weight of core−core correlation energy (cc-pwCV*n*Z). Due to the correlation of 3d orbitals, added shells of higher angular momentum exponents compared to the valence sets are necessary to describe the core region. The pattern of added core-correlating functions is (1s1p1d1f) for double-ζ, (2s2p2d2f1g) for triple-ζ, (3s3p3d3f2g1h) for quadruple-ζ, and (4s4p4d4f3g2h1i) for quintuple-ζ. Atomic and molecular results show good convergence to the CBS limit, with the cc-pwCV*n*Z sets showing improved convergence compared to the cc-pCV*n*Z ones for molecular core−valence correlation effects. After testing the basis sets on the homonuclear diatomics Ga_2−Kr_2 with coupled cluster wave functions, it is concluded that a treatment of core−valence correlation effects is essential for high-accuracy ab initio investigations of third-row-containing molecules. Though the basis sets are optimal for 3s3p3d correlation, preliminary atomic and molecular results show the basis sets to be efficient with respect to *3*d-only correlation, and these potentially could be used with 3d-only correlation for more qualitative studies on larger species.

Introduction

The two primary considerations to be made when numerically solving the electronic Schrödinger equation for an atomic or molecular system (with standard molecular orbital theories) are (a) the treatment of the spatial distribution of the electrons through selection of a one-electron basis set and (b) the description of the many-body interactions of N electrons, or electron correlation, through selection of a wave function representation. As is well-known, basis sets approaching completeness are computationally intractable, and traditional molecular orbital (MO)-based wave function methods formally scale as, at least, N^4 with respect to the basis set size. The errors arising from the basis set and wave function choices are inherently coupled, and this coupling also interplays with computational tractability.

With the development of systematically convergent families of basis sets, the complete basis set (CBS) limit can be approached through mathematical extrapolation. The correlation consistent basis sets, first developed by Dunning,[1] have allowed the complex interplay between the basis set quality and wave function ansatz to be unraveled. When the CBS limit of a calculated quantity is known, the error remaining corresponds to the intrinsic error in the chosen electronic structure method. By systematically expanding the treatment of radial space and angular momentum, the correlation consistent basis sets approach the CBS limit as the basis set size increases toward infinity.

Construction of the correlation consistent basis sets begins with a set of primitive, generally contracted Gaussian-type functions to describe the atomic Hartree−Fock orbitals. From there, higher angular momentum functions are grouped according to their contribution toward the atomic correlation energy and are then added in shells. The correlation consistent basis sets are usually named according to their zeta level, denoted by cc-pV*n*Z, where *n* is the zeta level (n = D for double-ζ, T for triple-ζ, Q, 5, etc.) It has been found that the convergence behavior of many atomic and molecular quantities is regular and monotonic when they are determined from a sequence of calculations employing increasing values of n.[2−6]

Correlation consistent polarized valence basis sets (cc-pV*n*Z) exist for first-,[1] second-, and third-row elements[7−9] and have been augmented with diffuse functions (aug-cc-pV*n*Z),[10,11] were recontracted using the spin-free, one-electron Douglas−Kroll−Hess (DKH) Hamiltonian[12−14] to describe scalar relativistic effects (cc-pV*n*Z-DK),[15,16] and have been constructed with pseudopotentials[17−20] (cc-pV*n*Z-PP) and all-electron forms for heavy elements and the treatment of transition-metal-containing systems.[19,21] First- and second-row correlation consistent basis sets were modified to account for core−valence electron correlation (cc-pCV*n*Z and cc-pwCV*n*Z).[19−23] The treatment of core−valence (CV) electron correlation is necessary when high

† Part of the "Thom H. Dunning, Jr., Festschrift".

‡ University of North Texas.
§ Washington State University.
£ E-mail: akwilson@unt.edu.
E-mail: kipeters@wsu.edu.

10.1021/jp0747757 CCC: $37.00
Published on Web 10/06/2007

accuracy is desired for the calculation of spectroscopic and energetic properties. It is well-known that core−valence effects can increase with increasing molecular size and are often more substantial in systems containing heavier elements. For example, current ab initio composite methods in use, such as G3 and its variants,[24−28] the correlation consistent composite approach (ccCA),[16,29,30,31] the complete basis set (CBS-*n*) approaches of Petersson and co-workers,[32−35] the focal point method of Allen, Császár, and co-workers,[36−43] the W*n* methods of Martin and de Oliveira,[44−47] the HEAT method of Stanton and co-workers,[48−50] and the additive coupled cluster approach of Dixon, Feller, Peterson, and co-workers[51−61] ubiquitously include corrections for CV effects.

While a complete suite of Pople-style split-valence basis sets is available for third-row p-block species (Ga−Kr),[28,62−64] which inherently provide some description of 3d correlation effects, core−valence correlation consistent basis sets have not yet been uniformly constructed for these elements, nor have the effects of CV correlation within the all-electron cc-pV*n*Z family of basis sets been thoroughly investigated on energetic or structural properties of molecules containing third-row elements, except for a few specific applications.[59,60,65−68] It is the goal of this investigation to provide new core−valence correlation consistent basis sets to complete the full "suite" of basis sets for the elements Ga−Kr. The effects of core−valence correlation on the bond lengths, vibrational frequencies, and dissociation energies of the homonuclear dimers of these six elements will also be examined.

Methodology

The MOLPRO 2006.1 software package has been used exclusively in this study. Basis set construction and optimization followed the general format of the 3d transition-metal basis set construction carried out by Balabanov and Peterson.[21] Basis function exponents were optimized employing a conjugate gradient algorithm[69] using double-sided numerical derivatives with energy gradients converged to 1×10^{-6} Hartrees or better. Only the pure spherical harmonic components were used. To determine the optimal exponents for core and core−valence basis functions, atomic computations were carried out using configuration interaction with single and double substitutions (CISD) to the reference wave function. When degeneracy occurred within the atomic ground states (for Ga, Ge, Se, and Br), a state-averaged HF wave function was used to ensure symmetry equivalence.[21,22] The degeneracy of the ensuing orbitals is not strictly enforceable on the CISD wave functions, but the effect of this symmetry breaking is expected to be small. Subsequent benchmark calculations were carried out using the coupled cluster method with single, double, and perturbative triple excitations [CCSD(T)].[70] All open shell CCSD(T) computations were obtained with restricted open-shell HF (ROHF) orbitals, state-averaged for symmetry equivalencing, but allowed for small amounts of spin contamination in the solution of the CCSD equations, that is, R/UCCSD(T).[71,72]

Core and Core−Valence Correlation in Third-Row Atoms Ga−Kr

A. Establishing Correlation Consistency. The definition of the core electron space for the atoms Ga−Kr is somewhat more involved than that with the previous core−valence basis sets since the valence-correlation consistent basis sets were constructed with the 3d electrons frozen.[8] In keeping with the methodology of correlation consistent basis set, only the $(n - 1)$ shell will be included in the correlation treatment, that is, the K and L shells ($1s^2 2s^2 2p^6$) will be treated with the frozen-core approximation. The core and valence orbitals to be correlated will then include just the M ($3s^2 3p^6 3d^{10}$) and N shell (valence $4s^2 4p^6$) electrons, and the term all-electron will refer to the inclusion of just these M and N shell MOs. In order to avoid potential confusion between the Barka shell notation and other quantum numbers, electron correlation is divided into three separate classes, core−core correlation (CC), core−valence correlation (CV), and valence−valence (VV) correlation. An all-electrons-correlated calculation would thus equal the sum of the CC, CV, and VV contributions (assuming size extensivity).

During the construction of the first-row CV basis sets (B−Ne), it was determined that correlation consistent shells of basis functions could lead to systematic convergence of the core−core electron correlation energy.[22] Optimizing functions for core−core correlation was based on the hypothesis that basis functions describing core−valence (intershell) correlation effects would be bracketed by functions describing the core−core and valence−valence effects, yielding a systematic convergence to the CBS limit as both the augmenting core function sets and original valence sets were increased in size. However, a better-behaved convergence to the CBS limit was obtained when the additional core-correlating functions were optimized for the difference between the all-electron and frozen-core calculations. Using CISD wave functions on the third-row atoms, this is described as

$$\Delta E_{\mathrm{corr}} = E_{\mathrm{CISD}}(\mathrm{CC} + \mathrm{CV} + \mathrm{VV}) - E_{\mathrm{CISD}}(\mathrm{VV}) \qquad (1)$$

Initial basis set optimizations were carried out for the selenium atom in the same manner as those for the second-row atom core−valence work.[23] As in the construction of the valence basis sets for the third-row atoms and first-/second-row core−valence basis sets, the other atoms in the third-row p-block were expected to have behavior analogous to that of selenium. The initial exponent optimizations were carried out by minimizing the correlation energies (with a 3s3p3d core definition) via eq 1 and were based on a partially uncontracted cc-pVQZ basis, (21s16p9d)/[9s8p1d]. From one to six d-type functions were then added to this set and optimized. Next, one to six f-type functions were added to the (21s16p14d)/[9s8p6d] set, and the exponents were optimized; one to five optimized g-type functions were added to the resulting (21s16p14d5f)/[9s8p6d5f] set, one to three h-type functions were added to the (21s16p14d5f4g)/[9s8p6d5f4g] set, and finally one to two i-type functions were added to the (21s16p14d5f4g3h)/[9s8p6d5f4g3h] set.

Incremental contributions to the CC + CV correlation energy are presented in Figures 1 (for d, f, g, h, i functions) and 2 (for s and p functions). As in the prior valence and core−valence correlation consistent basis sets, correlation energy convergence is monotonic with respect to increasing basis set size. However, unlike the valence third-row p-block and the second-row core−valence groupings, d- and f-type functions generally contribute a similar amount of correlation energy, and the fifth f function (and beyond) with a (5d5f) or (5d6f) grouping contributes more correlation energy than the corresponding fifth or sixth d function. The larger or nearly equivalent energy contribution of f-type functions compared to those of d-type holds true when only the 3d electrons are included in the core. Thus, our core−valence correlation groupings should be (1d1f), (2d2f1g), (3d3f2g1h), and (4d4f3g2h1i). With these groupings, the core−valence component of third-row species more closely resembles the 3d transition-metal valence basis sets than the second-row

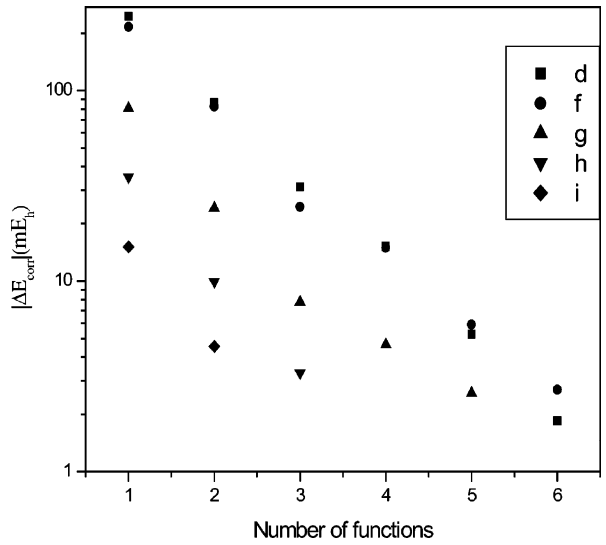

Figure 1. Incremental contributions of polarization functions to the Se CC + CV correlation energy. The absolute values are plotted against the number of functions in an even-tempered expansion for d, f, g, h, and i functions and are given in units of mE_h.

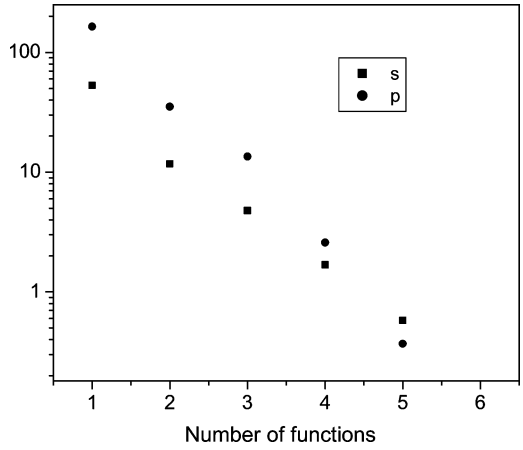

Figure 2. Incremental contributions of s- and p-correlating functions to the Se CC + CV correlation energy. The absolute values are given in units of mE_h.

CV basis sets. These are also consistent with the core−valence basis sets for Ga developed previously by Bauschlicher,[73] as well as those for Ga and Ge by Martin and Sundermann.[74] Higher angular momentum functions are somewhat more important than saturation of lower *l*-valued core functions, for example, the first h function contributes more correlation energy than the second g function, and the first i function contributes more to the correlation energy than the third g function or second h function. This phenomenon is observed in all currently constructed valence and core−valence correlation consistent basis sets. It is worth mentioning that the core−valence correlation consistent basis sets for Ga−Kr will have a maximum basis set angular momentum (l_{max}) that is one greater than the cardinal number or zeta level, that is, the cc-pCVDZ basis sets will have $l_{max} = 3$ but a cardinal number $n = 2$. This will affect certain types of CBS extrapolation formulas that depend explicitly on l_{max}.

The s and p core-correlating functions were optimized in a similar fashion as the higher angular momenta. For the s functions, a (21s16p17d3f) primitive set was contracted to [4s9p6d3f], and exponents of one to five s functions were varied to minimize the (CC + CV) CISD correlation energy. The p functions were similarly optimized in a [10s3p6d3f] basis set.

TABLE 1: Contraction Schemes for the Third-Row Valence Basis Sets and Added Core−Valence Correlation Basis Functions

set	cc-pV*n*Z	*N*	cc-p(w)CV*n*Z	*N*
DZ	[5s4p2d]	27	+(1s1p1d1f)	43
TZ	[6s5p3d1f]	43	+(2s2p2d2f1g)	84
QZ	[7s6p4d2f1g]	68	+(3s3p3d3f2g1h)	145
5Z	[8s7p5d3f2g1h]	104	+(4s4d4f3g2h1i)[a]	227

[a] The original HF *p* set was recontracted. See text.

The incremental energy contributions of the added s and p functions are shown in Figure 2. As with the first- and second-row core−valence basis sets, the incremental contributions of s functions tail off rather quickly, while the contributions of p functions decrease more slowly. Unlike the previous core−valence basis sets for the first and second rows, the convergence behavior of the p functions resembles that of the s functions more than that of the d functions and fall off much faster after the fourth p function is added. Still, the s and p components of the CV basis sets were constructed in a manner akin to the previous correlation consistent CV sets, that is, (1s1p) was paired with the (1d1f) group of functions to form the core−valence cc-pCVDZ set, the (2s2p) set was paired with the (2s2f1g) set to form the cc-pCVTZ set, and so forth.

B. The cc-pCV*n*Z and cc-pwCV*n*Z Basis Sets for Ga−Kr. Once the sets of additional core functions were determined for each zeta level using the selenium atom as an example, the augmenting core functions were optimized using eq 1 for the remaining five elements. Just as with Se, these functions were optimized in the presence of the corresponding valence basis set. Analogous to the second-row core−valence basis sets,[23] one exception was required for the cc-pCV5Z basis sets. Because the p-type exponents were optimized in CISD calculations rather than just uncontracting primitive functions from the HF sets, strong linear dependencies arose between the optimized correlating p functions and those within the HF sets at the quintuple-ζ level. In these cases, the cc-pV5Z (26s17p)/[8s7p] sets were recontracted to [8s10p], where the eight most diffuse p functions were left uncontracted. The remaining (4s4d4f3g2h1i) functions were then added together with the original valence-correlating functions to form the cc-pCV5Z basis sets. The compositions and sizes of the resulting cc-pCV*n*Z basis sets are given in Table 1, and the optimized exponents are given explicitly as Table S1 of the Supporting Information.[75]

Another issue that arose when optimizing the cc-pCV*n*Z basis sets was two strongly competing minima for the s-type functions, one minimum having a tighter set of exponents and the other minimum having a more diffuse set. Energetic differences between the two were minimal in the sub-mE_h range for cc-pCVDZ sets and decreasing to the μE_h range for cc-pCV5Z. Convergence of molecular properties at the CBS limit seemed to be alleviated of some linear dependency issues when the more diffuse s set was used for cc-pCVDZ and cc-pCVTZ and the tighter s set for cc-pCVQZ and cc-pCV5Z basis sets. In essence, this makes the s functions of the cc-pCV*n*Z basis sets more resemble the s functions of the cc-pwCV*n*Z sets (see below), where the leading (or most diffuse) s-type function gradually becomes tighter upon increasing zeta level. This effect can be seen in Figure 3.

As in ref 23, the individual energy contributions (CC, CV, and VV) of the CISD all-electron calculations were assessed with respect to CBS convergence. In Figure 4, the contributions are shown for the cc-pCV*n*Z and cc-pV*n*Z basis sets for the selenium atom. As discussed previously,[23] the core−valence (or CV) contribution is not straightforward to assess since only

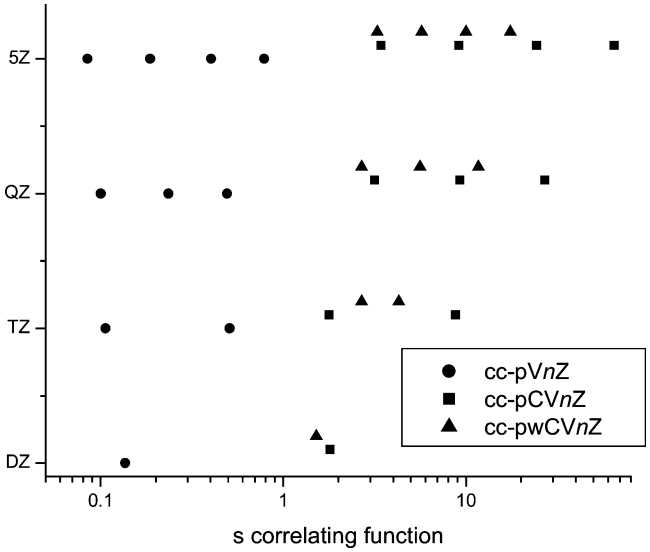

Figure 3. Values of the selenium atom s-function exponents within the even-tempered expansion.

double excitation contributions to the CV correlation energy can be directly computed within MOLPRO. The CV singles correlation energy has been approximated from the difference in singles-only calculations involving all-electron, CC-only, and valence-only calculations

$$E_{\mathrm{corr}}(\mathrm{CV,\ singles}) = E_{\mathrm{corr}}(\mathrm{all\text{-}electron,\ singles}) - E_{\mathrm{corr}}(\mathrm{CC,\ singles}) - E_{\mathrm{corr}}(\mathrm{VV,\ singles}) \quad (2)$$

This result is then added to the CV pair-only correlation energy to yield the total intershell CV correlation energy. Since the CISD method is not size-extensive, the sum of the individual CC, CV, and VV contributions do not yield the all-electron CISD energy. This lack of size-extensiveness also prevents the CV correlation contribution from being computed simply as

$$E_{\mathrm{corr}}(\mathrm{CV}) = E_{\mathrm{corr}}(\mathrm{all}) - E_{\mathrm{corr}}(\mathrm{CC}) - E_{\mathrm{corr}}(\mathrm{VV})$$

As the singles contribution is generally less than 10% of the total magnitude of the CV contribution, this approximate description should not introduce significant errors.

Figure 4 clearly reveals monotonic convergence toward a CBS limit for each correlation energy contribution with the cc-pCV*n*Z basis sets. Using the valence cc-pV*n*Z basis sets in all-electron computations, however, shows an extremely poor convergence for both the CC and CV contributions, as well as a poor overall recovery of core−core and core−valence correlation energies. Therefore, the usual caveat applies in that conclusions about the effects of core electron correlation using only standard valence cc-pV*n*Z basis sets are probably invalid and, at best, a waste of computing resources.[22,23] *For all-electron computations, specially designed basis sets like the ones developed in this work are required for reliable results.* This is shown explicitly below for the case of the Ga_2 molecule.

Even more so than the second-row p-block atoms, the core−core correlation energy dominates the contributions to the all-electron correlation energy. For Se, the CC correlation energy was 825 mE_h at the cc-pCV5Z level, compared to 288 mE_h for the S atom. Our approximation of the total core−valence (CV) energy was 123 mE_h for Se, versus 58 mE_h for S. The core−core (CC) correlation energy of Se contributed 76% of the total correlation energy, which is essentially the same as the valence (VV) contribution for the oxygen atom! At the cc-pCVDZ level

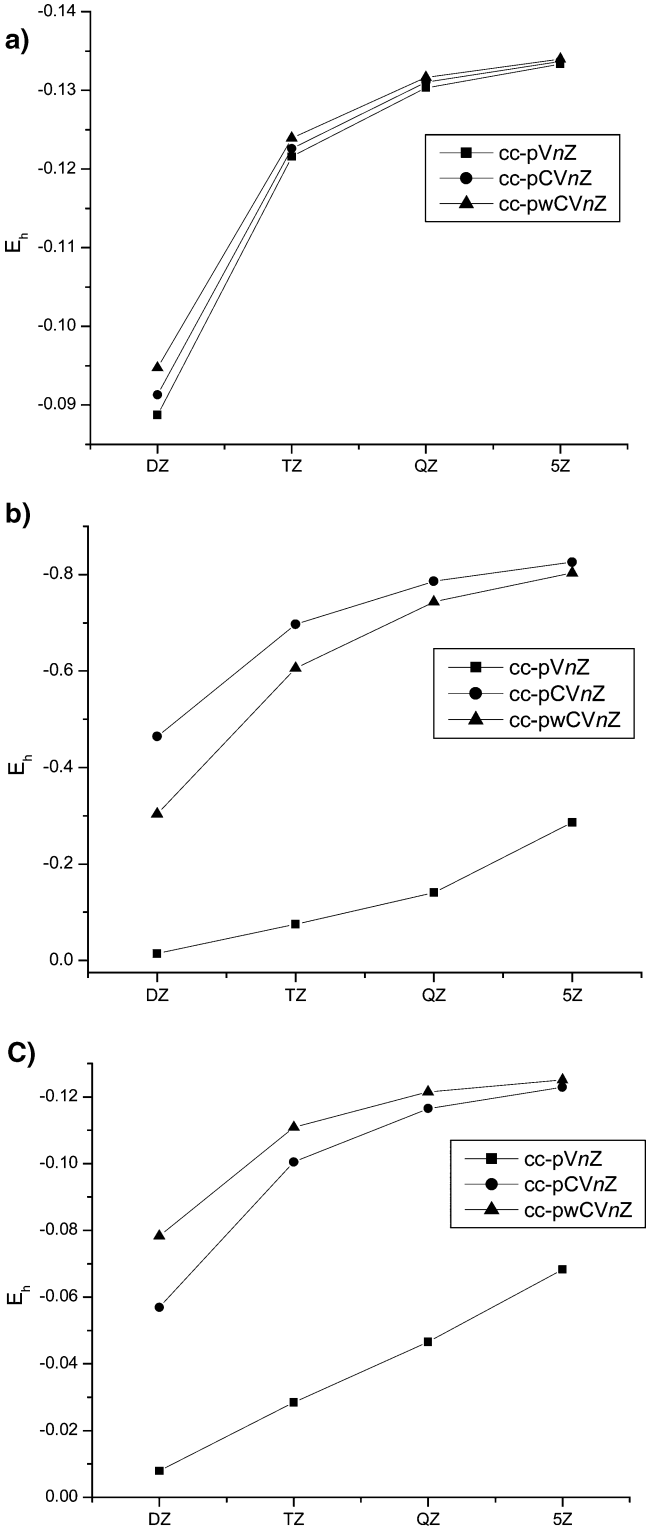

Figure 4. Representation of the (a) valence−valence correlation energy, (b) core−core correlation energy, and (c) core−valence correlation energy for the selenium atom using the cc-pV*n*Z, cc-pCV*n*Z, and cc-pwCV*n*Z basis sets.

of theory, 56% of the Se E_{corr}(CC) was recovered (versus 61% for cc-pCVDZ sulfur), and 46% of the Se E_{corr}(CV) was recovered versus 48% for S atom.

As for the first- and second-row atoms, as well as the 3*d* transition metals, a set of weighted core−valence basis sets was also developed for the atoms Ga−Kr. The motivation for the creation of the cc-pwCV*n*Z basis sets was to improve the CBS convergence of the intershell (CV) correlation energy. This was

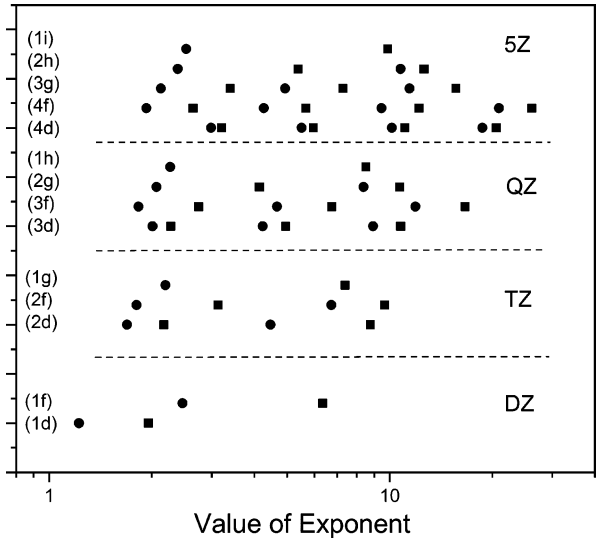

Figure 5. Pictorial comparison of cc-pCV*n*Z (squares) and cc-pwCV*n*Z (circles) optimized exponents of higher angular momentum core functions for the selenium atom.

carried out by strongly weighting core−valence correlation versus core−core (CC) correlation. While the CC correlation would more slowly converge to its CBS limit, the CV correlation contribution, which is expected to be more important to most atomic and molecular properties, would converge more rapidly. The same groupings of functions used above for the cc-pCV*n*Z basis sets were used, but the CISD energy was optimized with

$$\Delta E_{\mathrm{CISD}}(\mathrm{CV} + w\mathrm{CC}) = E_{\mathrm{CISD}}(\mathrm{CV}) + wE_{\mathrm{CISD}}(\mathrm{CC})$$

where w is a weighting factor and E_{CISD}(CV) was obtained from the CV doubles contribution plus eq 2 for the singles. A value of $w = 0.01$ was used, as it was previously found to provide exponents that converge the CC contribution of the correlation energy, as well as speed up the CV contribution relative to the cc-pCV*n*Z basis sets.[22] The optimized exponents of the cc-pwCV*n*Z are also given in Table S1 of the Supporting Information. The convergence of each correlation energy component with the cc-pwCV*n*Z basis sets is also shown in Figure 4. The faster convergence of the CV component is clearly evident at the expense of the CC energy.

A comparison of the exponent distributions of core-correlating functions for the Se atom between the cc-pCV*n*Z and cc-pwCV*n*Z basis sets is given in Figure 5. Exponents of the weighted sets tend to be more diffuse, much like the trend observed for the first- and second-row cc-pwCV*n*Z basis sets[23] and especially for the highest angular momentum function in each set, for example, the f function of the DZ sets or the g function of the QZ sets. As the basis set sizes increase from DZ to 5Z, the values of cc-pCV*n*Z and cc-pwCV*n*Z exponents become more similar. Differences in the resulting core−valence correlation effects on energetics and properties of third-row-containing molecules will be investigated below.

Results and Discussion for the Homonuclear Dimers Ga_2 through Kr_2

Benchmark calculations of the new Ga−Kr core−valence basis sets were carried out for the six respective homonuclear diatomics using the CCSD(T) level of theory. Dissociation energies (D_e), equilibrium geometries (r_e), and harmonic vibrational frequencies (ω_e) were determined and compared to experiment and previous theoretical studies. Whenever necessary, computed zero-point energies (ZPE) and spin−orbit coupling corrections were added to dissociation energies in order to properly compare computed D_e to experimental D_0 values. The spectroscopic properties for the ground states of the homonuclear diatomics are listed in Tables 2−9 (along with a low-lying excited state of Ge_2 in Table 5). Since scalar relativistic effects are known to be important in accurate work on these species, the Douglas−Kroll−Hess Hamiltonian was employed throughout.[12−14] As in previous work for these elements, the nonrelativistic exponents of the basis sets were used unchanged, but contraction coefficients were replaced with those from atomic DKH calculations.[12−14] The resulting aug-cc-pV*n*Z-DK, aug-cc-pCV*n*Z-DK, and aug-cc-pwCV*n*Z-DK basis sets will be denoted below as aV*n*Z-DK, aCV*n*Z-DK, and awCV*n*Z-DK, respectively.

A. Ga_2. The electronic structure of the gallium dimer is well-known both experimentally[76−78] and theoretically,[79,80] with a ground state of $^3\Pi_u$. Recent work on this molecule includes theoretical multireference wave function studies by Mochizuki and co-workers[81] and Roos, Widmark, and co-workers,[82] a Knudsen cell mass spectrometric study of Ga_2 dissociation energies by Meloni and co-workers,[83] investigations of the laser-induced fluorescence spectrum of Ga_2 by Tam and Dagdigian[84] and Greetham and Ellis[85] that provides direct experimental evidence of the $^3\Pi_u$ ground state and updated spin−orbit splitting assignments, and a matrix-isolation study by Himmel and Gaertner that provides a vibrational anharmonicity constant.[86]

Computed spectroscopic properties of $X^3\Pi_u$ Ga_2 are shown in Table 2. Valence−valence correlation effects of the added basis functions within the aCV*n*Z-DK and awCV*n*Z-DK sets are minimal compared to those of the original aV*n*Z-DK sets and show smooth, monotonic convergence to a CBS limit. When only 4s4p valence electrons are correlated, Ga_2 D_e and ω_e values are essentially converged to the same values when using the valence, CV, and wCV basis sets at the 5Z level, while r_e values agree among the various basis sets to within 0.003 Å. For energetic properties, it is apparent that inclusion of core−valence effects is necessary for chemical accuracy (defined as being within 1 kcal mol^{-1} of an experimental value for energetic properties). At the quintuple-ζ level, the shift in D_e from 3s3p3d correlation is +1.2 kcal mol^{-1}. Core−valence correlation shortens bond lengths by ~0.07 Å, resulting in a 6.2 cm^{-1} increase in ω_e. For Ga_2 (and the five other homonuclear diatomics), there do not appear to be qualitative differences between the aCV*n*Z-DK and awCV*n*Z-DK families of basis sets, although the convergence with basis set is clearly faster with the awCV*n*Z-DK sets, especially for the bond length.

The detrimental effects of correlating the 3s3p3d electrons with just the valence aug-cc-pV*n*Z-DK basis sets are clearly observed. For bond distances, non-monotonic convergence to a CBS limit is shown, and the aV5Z-DK r_e value is more than 0.10 Å shorter than the aVQZ-DK value when only valence electrons are correlated. The aV*n*Z-DK all-electron ω_e values are substantially larger than the experimental value and show non-monotonic convergence as well. Core−core and core−valence correlation effects are greatly overestimated by the aV*n*Z-DK sets, as shown by the dramatic overestimation of D_e, where the +3s3p3d aV5Z-DK value is 4.6 kcal mol^{-1} higher than the valence value. As mentioned previously, using valence correlation consistent basis sets to describe CC and CV correlation can produce unreliable results.

Using the theoretical molecular spin−orbit (SO) coupling correction obtained in a study by Das using multireference

TABLE 2: Properties for Ga_2 ($X^3\Pi_u$)

	D_e (kcal/mol)			r_e (Å)			ω_e (cm^{-1})		
basis	4s4p	+3s3p3d	Δ	4s4p	+3s3p3d	Δ (mÅ)	4s4p	+3s3p3d	Δ
aVDZ-DK	26.2	29.4	3.2	2.7605	2.7044	−56.2	160.5	170.7	10.2
aVTZ-DK	29.0	35.2	6.2	2.7352	2.6022	−133.1	165.2	181.8	16.6
aVQZ-DK	29.6	36.2	6.7	2.7281	2.6159	−112.2	166.2	181.2	15.1
aV5Z-DK	29.7	34.3	4.6	2.7273	2.6204	−106.9	166.7	187.3	20.6
aCVDZ-DK	26.4	28.5	2.1	2.7549	2.7131	−41.7	161.2	168.0	6.7
aCVTZ-DK	29.1	30.8	1.7	2.7332	2.6709	−62.3	165.8	172.6	6.8
aCVQZ-DK	29.6	30.9	1.3	2.7263	2.6589	−67.4	166.4	172.1	5.7
aCV5Z-DK	29.9	31.1	1.2	2.7249	2.6536	−71.3	167.0	173.2	6.2
awCVDZ-DK	26.7	28.4	1.7	2.7459	2.6877	−58.2	161.8	167.7	5.9
awCVTZ-DK	29.2	30.6	1.4	2.7310	2.6629	−68.1	166.2	172.7	6.6
awCVQZ-DK	29.7	30.9	1.2	2.7254	2.6532	−72.2	166.6	172.8	6.2
awCV5Z-DK	29.9	31.1 (D_0 = 30.9)	1.2	2.7244	2.6510	−73.4	167.1	173.3	6.2
ANO CASPT2[a]		D_0 = 26.1 (28.6)[b]			2.697			191	
expt.		D_0 = 26.4 ± 1.7[c] (D_e = 28.9)[b]						178.2[d]	

[a] Ref 82. [b] Values in the parentheses have SO-coupling values removed from the dissociation energy. [c] Ref 80. [d] Ref 86, obtained from an argon matrix-isolation experiment.

TABLE 3: Differential Effects of 3s3p and 3d Correlation for Ga_2[a]

	D_e (kcal/mol)			r_e (Å)			ω_e (cm^{-1})		
basis	4s4p3d	Δ_{3d}	Δ_{3s3p}	4s4p3d	Δ_{3d} (mÅ)	Δ_{3s3p} (mÅ)	4s4p3d	Δ_{3d}	Δ_{3s3p}
aVDZ-DK	28.4	2.2	1.0	2.7184	−42.1	−14.1	168.6	8.1	2.1
aVTZ-DK	33.2	4.2	2.0	2.6376	−97.6	−35.4	177.9	12.6	4.0
aVQZ-DK	34.7	5.1	1.6	2.6285	−99.6	−12.6	181.3	15.1	0.0
aV5Z-DK	32.8	3.1	1.5	2.6297	−97.5	−9.3	183.0	16.3	4.4
aCVDZ-DK	28.2	1.8	0.3	2.7106	−44.2	2.5	167.6	6.4	0.3
aCVTZ-DK	30.8	1.8	0.0	2.6674	−65.7	3.5	173.0	7.3	−0.5
aCVQZ-DK	31.1	1.4	−0.2	2.6551	−71.2	3.8	172.7	6.3	−0.6
aCV5Z-DK	31.2	1.4	−0.1	2.6499	−75.0	3.7	173.8	6.8	−0.6

[a] Calculated using the 4s4p and +3s3p3d results of Table 2.

TABLE 4: Ge_2 Properties ($X^3\Sigma_g^-$)

	D_e (kcal/mol)			r_e (Å)			ω_e (cm^{-1})		
basis	4s4p	+3s3p3d	Δ	4s4p	+3s3p3d	Δ (mÅ)	4s4p	+3s3p3d	Δ
aCVDZ-DK	55.8	57.6	1.9	2.4212	2.4062	−15.1	276.6	280.6	4.0
aCVTZ-DK	62.0	63.7	1.7	2.4051	2.3779	−27.2	282.0	287.1	5.1
aCVQZ-DK	64.1	65.6	1.5	2.3998	2.3679	−31.9	284.3	289.4	5.1
aCV5Z-DK	64.8	66.3	1.5	2.3991	2.3644	−34.7	284.7	290.4	5.7
awCVDZ-DK	56.4	58.1	1.7	2.4149	2.3912	−23.8	277.3	281.3	3.9
awCVTZ-DK	62.2	63.8	1.6	2.4034	2.3715	−31.9	282.6	287.8	5.2
awCVQZ-DK	64.2	65.7	1.5	2.3991	2.3643	−34.8	284.7	290.4	5.7
awCV5Z-DK	64.8	66.4 (D_0 = 66.0)	1.5	2.3988	2.3626	−36.2	284.8	291.0	6.2
ANO CASPT2[a]		D_0 = 61.6 (67.0)[b]			2.362			287	
expt.[c]		D_0 = 62.3 ± 1.7[b] (67.7)			2.368				
expt.[d]					r_0 = 2.3689			287.9	

[a] Ref 82 (incorrectly labeled as the $^1\Sigma^+$ ground state; cf. Table 9). [b] Values in the parentheses have SO-coupling values removed from the dissociation energy. [c] Ref 91. [d] Ref 93.

configuration interaction and a relativistic core potential,[87] as well as the atomic spin−orbit splitting from Moore,[88] a SO correction can be "unfolded" from the experimental D_0 value to compare with our theoretical one. Adding these corrections to the experimental D_0 value of Shim[80] (26.4 ± 1.7 kcal mol^{-1}) gives an estimated experimental D_0 without SO of 28.9 kcal mol^{-1}. The aCV5Z-DK/awCV5Z-DK values are 30.9 kcal mol^{-1} after including a shift of −0.2 kcal mol^{-1} for ZPE, and these values are slightly outside of the experimental error bars. The D_0 values obtained when only correlating the valence electrons are smaller by 1.2 kcal/mol. Our best D_0 values are 1.2 kcal mol^{-1} larger than the value obtained by Widmark and co-authors,[82] as well as 1.4 kcal mol^{-1} larger than a value predicted by Mochizuki using the multireference coupled pair approximation and a segmented Huzinaga basis set of double-ζ size.[81] Although no experimental bond distance information is available, the aCV5Z-DK/awCV5Z-DK values are shorter than the r_e value from Widmark. Our quintuple-ζ harmonic frequencies are ∼4 cm^{-1} smaller than the best experimental value, which comes from an argon matrix-isolation experiment.[86]

In Table 3, the effect of correlating only the 3d orbitals on Ga_2 with the aV*n*Z-DK and aCV*n*Z-DK basis sets are shown. For spectroscopic properties, the aV*n*Z-DK basis sets show poor accuracy and non-monotonic convergence to the CBS limit when

TABLE 5: Properties of the Lowest-Lying Ge_2 Excited State ($^3\Pi_u$)

	T_e (cm^{-1})			r_e (Å)			ω_e (cm^{-1})		
basis	4s4p	+3s3p3d	Δ	4s4p	+3s3p3d	Δ (mÅ)	4s4p	+3s3p3d	Δ
aCVDZ-DK	1009	867	−142	2.3255	2.3093	−16.2	293.1	298.6	5.5
aCVTZ-DK	769	592	−176	2.3068	2.2773	−29.5	299.4	307.2	7.8
aCVQZ-DK	761	585	−176	2.2992	2.2644	−34.8	302.9	310.9	7.9
aCV5Z-DK	777	597	−180	2.2980	2.2609	−37.1	305.6	312.5	7.0
awCVDZ-DK	1033	840	−193	2.3182	2.2916	−26.6	293.4	299.6	6.2
awCVTZ-DK	785	607	−178	2.3047	2.2700	−34.7	299.7	307.9	8.1
awCVQZ-DK	772	596	−176	2.2986	2.2609	−37.7	303.2	311.8	8.5
awCV5Z-DK	783	607	−177	2.2973	2.2583	−39.0	303.9	312.8	8.9
MRCID[a]	323				2.33			313	
expt.[b]	725 (728)							(308)?	
expt.[c]	T_0 = 711								

[a] Ref 94 using the G2 basis sets of Binning and Curtiss.[112] [c] Ref 95. [d] Ref 93.

TABLE 6: Properties of As_2 ($X^1\Sigma_g^+$)

	D_e (kcal/mol)			r_e (Å)			ω_e (cm^{-1})		
basis	4s4p	+3s3p3d	Δ	4s4p	+3s3p3d	Δ (mÅ)	4s4p	+3s3p3d	Δ
aCVDZ-DK	72.0	73.8	1.8	2.1428	2.1347	−8.1	412.6	417.2	4.6
aCVTZ-DK	82.3	84.4	2.1	2.1265	2.1097	−16.8	422.4	430.0	7.6
aCVQZ-DK	86.7	88.9	2.2	2.1205	2.0999	−20.6	427.3	435.6	8.3
aCV5Z-DK	88.2	90.5	2.3	2.1187	2.0960	−22.7	428.6	437.6	9.0
awCVDZ-DK	73.0	74.9	1.9	2.1370	2.1228	−14.2	413.7	419.5	5.8
awCVTZ-DK	82.8	85.4	2.6	2.1253	2.1053	−20.0	423.5	432.2	8.7
awCVQZ-DK	86.9	89.2	2.2	2.1198	2.0972	−22.6	427.7	436.7	9.0
awCV5Z-DK	88.3	90.6 (D_0 = 90.0)	2.3	2.1185	2.0947	−23.7	428.9	438.4	9.5
aug-cc-pVnZ CCSD(T)[a]		90.3			2.126				
ANO CASPT2[b]		D_0 =86.9			2.133			413	
expt.[c]		D_0 = 90.6			2.103			429.6	

[a] Ref 98. [b] Ref 82. [c] Ref 76.

TABLE 7: Properties of Se_2 ($X^3\Sigma_g^-$)

	D_e (kcal/mol)			r_e (Å)			ω_e (cm^{-1})		
basis	4s4p	+3s3p3d	Δ	4s4p	+3s3p3d	Δ (mÅ)	4s4p	+3s3p3d	Δ
aCVDZ-DK	69.4	70.6	1.2	2.2046	2.1993	−5.3	371.3	373.7	2.3
aCVTZ-DK	76.3	77.6	1.3	2.1866	2.1753	−11.3	381.3	385.1	3.7
aCVQZ-DK	79.8	80.9	1.1	2.1783	2.1644	−13.9	387.4	391.5	4.2
aCV5Z-DK	81.0	82.1	1.1	2.1757	2.1603	−15.4	388.7	393.2	4.5
awCVDZ-DK	69.5	70.4	1.0	2.1991	2.1904	−8.8	372.4	375.0	2.6
awCVTZ-DK	76.6	77.9	1.2	2.1841	2.1706	−13.5	382.0	386.1	4.1
awCVQZ-DK	79.9	80.9	1.0	2.1775	2.1622	−15.2	387.7	392.2	4.4
awCV5Z-DK	81.1	82.1 (D_0 = 81.6)	1.0	2.1752	2.1593	−15.8	388.9	393.6	4.8
ANO CASPT2[a]		D_0 = 79.1 (84.5)[b]			2.180			384	
SDB−PP CCSD(T)[c]		77.0			2.1830			389.6	
6-31G* B3LYP[d]					2.191			390	
expt.[e]		D_0 = 78.6 (84.0)			2.166			385	
expt.[f]					2.1662			386.6	

[a] Ref 82. [b] Values in the parentheses have SO-coupling values removed from the dissociation energy. [c] Ref 74. [d] Ref 101. [e] Ref 76. [f] Ref 103.

the 3d MOs are added to the electron correlation space. As shown with the aCVnZ-DK basis sets, correlation of the 3s and 3p electrons does not have a significant effect on the computed properties. Though the family of cc-pCVnZ sets was constructed and optimized to correlate the 3s3p3d electrons, it was observed that Se exponents optimized for just 3d-only correlation were quite similar to the ones obtained with 3s3p3d correlation. At the quintuple-ζ level, the effects of 3s3p correlation shift D_e by just −0.1 kcal mol^{-1}, r_e by +0.0037 Å, and the value of ω_e by −0.6 cm^{-1}. Hence, the majority of the total core−valence correlation effects on these properties arises from 3d electron correlation. For high-accuracy energetic and geometric analysis of third-row-containing species utilizing CBS extrapolations, correlation of the 3s3p will still be necessary. However, for qualitative studies on larger molecules where only double- or triple-ζ level computations may be tractable, utilizing the pCVnZ and pwCVnZ sets with 3d4s4p-correlated MOs is likely to be useful for efficiently gauging CV correlation effects.

B. Ge_2. Although the ground electronic state of Ge_2 is well-established as $X^3\Sigma_g^-$,[89−91] it has historically been a difficult molecule to study experimentally (due to the large relative abundances of its various isotopic forms) and theoretically (due

TABLE 8: Properties of Br_2 ($X^1\Sigma_g^+$)

	D_e (kcal/mol)			r_e (Å)			ω_e (cm^{-1})		
basis	4s4p	+3s3p3d	Δ	4s4p	+3s3p3d	Δ (mÅ)	4s4p	+3s3p3d	Δ
aCVDZ-DK	40.6	41.3	0.7	2.3444	2.3402	−4.3	295.1	296.3	1.3
aCVTZ-DK	47.7	48.4	0.6	2.3080	2.2988	−9.1	316.6	319.1	2.6
aCVQZ-DK	50.4	50.8	0.4	2.2949	2.2837	−11.2	324.2	327.2	3.0
aCV5Z-DK	51.4	51.7	0.3	2.2913	2.2791	−12.3	326.3	329.6	3.3
awCVDZ-DK	40.8	41.3	0.5	2.3388	2.3315	−7.3	295.4	297.2	1.9
awCVTZ-DK	47.9	48.4	0.5	2.3058	2.2949	−10.9	316.6	319.6	2.9
awCVQZ-DK	50.5	50.7	0.2	2.2941	2.2820	−12.1	324.4	327.5	3.1
awCV5Z-DK	51.4	51.6 (D_0 = 51.1)	0.2	2.2910	2.2782	−12.7	326.2	329.5	3.4
ANO CASPT2[a]		D_0 = 41.5 (48.5)[b]			2.298			317	
CBS CCSD(T)[c]		D_0 = 45.4 (52.4)[b]			2.2816			330.3	
aug-cc-pV5Z-PP CCSD(T)[d]					2.292				
expt.[e]		D_0 = 45.44 (52.4)[b]			2.2810			325.3	

[a] Ref 82. [b] Values in the parentheses have SO-coupling values removed from the dissociation energy. [c] Ref 53. [d] Ref 98. [e] Refs 76 and 106. The results from these experimental papers agree within the number of significant digits reported in this table.

TABLE 9: Properties of Kr_2 ($X^1\Sigma_g^+$)

	D_e (kcal/mol)			r_e (Å)			ω_e (cm^{-1})		
basis	4s4p	+3s3p3d	Δ	4s4p	+3s3p3d	Δ (mÅ)	4s4p	+3s3p3d	Δ
aCVDZ-DK	0.26	0.34	0.09	4.2729	4.1814	−91.5	16.9	18.7	1.8
aCVTZ-DK	0.33	0.39	0.06	4.1246	4.0683	−56.3	21.3	23.2	1.9
aCVQZ-DK	0.38	0.39	0.00	4.0613	4.0216	−39.7	22.4	23.5	1.1
aCV5Z-DK	0.38	0.38	0.00	4.0486	4.0208	−27.8	23.0	23.7	0.7
awCVDZ-DK	0.24	0.30	0.06	4.2875	4.2405	−47.0	16.7	15.4	−1.4
awCVTZ-DK	0.33	0.38	0.05	4.1282	4.0875	−40.8	20.9	22.1	1.2
awCVQZ-DK	0.36	0.38	0.02	4.0635	4.0347	−28.8	22.3	23.0	0.7
awCV5Z-DK	0.38	0.39	0.02	4.0478	4.0249	−22.9	23.3	23.8	0.5
ANO CASPT2[a]		D_0 = 0.39			4.03			23	
"av5z+" CCSD(T)[b]		0.38			4.059				
CBS CCSD(T)[c]		0.36			4.08				
expt.[d]		0.362			4.04			23.8	
expt.[e]					4.017			23.5	

[a] Ref 82. [b] Ref 111. [c] Ref 110. [d] Ref 108. [e] ref 109.

to a very low-lying $^3\Pi$ state). Mass spectrometric[91,92] and laser-induced fluorescence[93] studies have provided accurate spectroscopic constants, while recent theoretical studies have examined the $1^3\Pi_u - X^3\Sigma_g^-$ excitation energy at various sophisticated levels of theory and found the transition energy (T_e) to be in the range of 0.04−0.10 eV (320−810 cm^{-1}).[92,94]

In Table 4, Ge_2 $X^3\Sigma_g^-$ spectroscopic properties obtained using the aCV*n*Z-DK and awCV*n*Z-DK basis sets are shown. As with the Ga_2 ground state, inclusion of core−valence correlation significantly contracts the bond length (−0.0347 to −0.0362 Å at the quintuple-ζ level) and increases ω_e (5.7−6.2 cm^{-1}). This bond length contraction is beneficial as quintuple-ζ level geometries are now within 0.01 Å of the experimental r_0 value obtained by Clouthier and co-workers.[93] Employing our ab initio value of the vibration−rotation interaction constant, α_e, of 8.1 MHz yields an ab initio r_0 that is slightly longer than r_e by 0.002 Å, which does result in better agreement with experiment. However, the final CCSD(T) r_0 is shorter than that of experiment by about 0.004 Å. Harmonic frequencies are in good agreement and slightly overshoot the experimental value by 2.5−3.0 cm^{-1}. On the basis of the experimental atomic SO splitting, as well as the molecular SO levels determined by Clouthier and co-workers,[93] the experimental D_0 value of 62.3 ± 1.7 kcal mol^{-1} can be shifted to a non-SO D_0 value of 67.7 kcal mol^{-1}. When corrected for ZPE effects, the aCV5Z-DK/awCV5Z-DK D_0 values are in good agreement.

Since the $1^3\Pi_u$ state of Ge_2 is accessible with a single reference wave function (by performing a $2\sigma_g \rightarrow 1\pi_u$ valence excitation), spectroscopic properties and transition energies from the ground state can be determined at the CCSD(T) level of theory and are shown in Table 5. The spin−orbit constant of the inverted $^3\Pi_u$ excited state has been determined by Weltner and co-workers in neon and argon matrix-isolation experiments, while[95] SO splittings for the ground state have been measured by Hostutler.[93] Currently, the best estimate of T_e from these two studies is 725−728 cm^{-1}. Valence results using the core−valence correlation consistent basis sets predict an adiabatic transition energy that is ∼65 cm^{-1} too high. Inclusion of core−valence correlation shifts T_e by −180 to −177 cm^{-1}. The transition energy appears to be very insensitive to the basis set size, varying by only 0−4 cm^{-1} when increasing from the triple-ζ to quintuple-ζ level. Equilibrium geometries of the $^3\Pi_u$ excited state are significantly shorter (∼0.01 Å) than earlier theoretical bond lengths using multireference wave functions and a basis set of approximate triple-ζ size.[94] Harmonic

vibrational frequencies are within 4 cm^{-1} of the matrix-isolation value of Hostutler.[93]

C. As_2. The ground state of the arsenic dimer is a closed-shell $X^1\Sigma_g^+$ configuration. Huber and Herzberg have compiled the definitive experimental spectroscopic information.[76] Theoretical studies with a sharper focus on the arsenic dimer rather than larger arsenic-containing clusters include an MRCISD study carried out by Shirley, Balasubramanian, Feng, and coauthors[96] and a study by Shen and Schaefer employing the CCSD level of theory with triple-ζ-sized basis sets.[97] Theoretical spectroscopic properties on As_2 were obtained in the benchmark calculations of the third-row valence cc-pV*n*Z and small-core relativistic pseudopotential basis sets performed by Yockel, Mintz, and Wilson[98,99] and the CASPT2 study of homonuclear dimers by Widmark and coauthors.[82]

Our frozen-core aCV5Z-DK and awCV5Z-DK results, presented in Table 6, are in close agreement with those acquired by Yockel and Wilson. The addition of core−valence correlation contracts the bond length by 0.022−0.024 Å, bringing it in closer agreement to the experimental value. Curiously, valence harmonic frequencies are within 1 cm^{-1} of the experimental ω_e, while the core−valence shift of +9.0 to +9.5 cm^{-1} at the quintuple-ζ level shows a greater deviation from experiment. The remaining error is presumably due to intrinsic errors in the CCSD(T) method. An experimental $\omega_e x_e$ has been determined (1.12 cm^{-1}), and our awCV5Z value of 0.99 cm^{-1} is in very good agreement. Theoretical calculation of the dissociation energy of As_2 is not complicated by spin−orbit coupling effects in the atom or molecule, and when our awCV5Z-DK D_e value is augmented by a ZPE correction, it is only lower than the experimental D_0 of 90.6 kcal/mol by 0.6 kcal/mol. It is expected that CBS extrapolations of the aug-cc-pwCV*n*Z energies should bring the final D_0 to within a few tenths of a kcal/mol of the experimental value. Last, the (frozen-core) value of $D_e = 90.3$ kcal mol^{-1} obtained by Yockel, Mintz, and Wilson may also be in fortuitous agreement with the experimental result[98] since our frozen-core aCV*n*Z-DK and awCV*n*Z-DK results are lower than their nonrelativistic aV*n*Z values but quite close to the value (within 0.1−0.2 kcal mol^{-1}) of Yockel and Wilson when relativistic aug-cc-pV5Z-PP basis sets were used.[99] The inclusion of core−valence correlation produces a shift of up to +2.3 kcal mol^{-1}. In this case, accounting for relativistic effects via the DK Hamiltonian seems to counteract the effect of core−valence correlation. However, our results are more theoretically rigorous and reliable than those of the previous study. It is also noteworthy to mention the deviation of more than 3 kcal mol^{-1} in the D_e calculation of Widmark and coauthors using a relativistic ANO basis set at the CASPT2 level of theory.[82]

D. Se_2. The Se_2 molecule has been extensively studied in the gas phase and is known to have a $^3\Sigma_g^-$ ground state.[76] A theoretical study of the ground state and many low-lying excited states was carried out by Balasubramanian.[100] More recently, Se_2 ground-state properties were obtained using a quadruple-ζ-sized Stuttgart−Dresden−Bonn pseudopotential (SDB−PP) created by Martin and Sundermann.[74] Equilibrium geometries and harmonic vibrational frequencies of the dimer and larger Se-containing clusters have also been studied using DFT.[101,102] Laser-excited fluorescence[103] and recent emission spectra have improved the quality of the Se_2 ground-state spectroscopic constants.[104,105]

Theoretical spectroscopic constants for the $X^3\Sigma_g^-$ state of Se_2 are reported in Table 7. The impact of core−valence correlation on the geometries is somewhat less for Se_2 than that for the previous homonuclear dimers. Using the aCV5Z-DK and awCV5Z-DK basis sets, there is an r_e shift of −0.0154 and −0.0158 Å, respectively. This shift brings the equilibrium geometries to within 0.006 Å of the experimental value, in better agreement compared to those of the ANO CASPT2 study of Widmark[82] and the 6-31G* B3LYP computations performed by Curtiss and co-workers.[101] Again, the frozen-core aCV5Z-DK and awCV5Z-DK harmonic frequencies are in fortuitously close concurrence with experiment, and the core−valence correlation shift of +4.5−+4.8 cm^{-1} yields final values from 6 to 7 cm^{-1} above the value of Vergès and co-workers.[103] The experimental dissociation energy can be "corrected" for molecular and atomic spin−orbit effects and estimated to be 84.0 kcal mol^{-1}. Corrected for ZPE, our best value is 81.6 kcal mol^{-1}, which is 1.0−1.1 kcal mol^{-1} closer to the experimental result than the frozen-core aCV5Z-DK and awCV5Z-DK values. This value is somewhat smaller in magnitude than the Widmark theoretical value,[82] but performing CBS extrapolations should only add 1−1.5 kcal mol^{-1} to the final D_0. Hence, the dissociation energy of this diatomic warrants further attention, including electron correlation beyond the CCSD(T) level of theory.

E. Br_2. The gaseous bromine dimer has a closed-shell $X^1\Sigma_g^+$ ground state and is well-described theoretically and experimentally. The report of Fosca, Li, and Bernath on the LIF spectra of the $B^3\Pi_u-X^1\Sigma_g^+$ electronic transition provides a comprehensive experimental history on the subject of Br_2 spectroscopy.[106] Recent theoretical work by Feller et al.,[53] Shepler and Peterson,[107] and Yockel, Mintz, and Wilson[98] provides accurate CCSD(T)/CBS spectroscopic constants, the former study using preliminary aCVQZ Br basis sets to account for core−valence correlation effects.

Similar to Se_2, calculation of molecular bromine equilibrium bond lengths (Table 8) shows a less pronounced influence from core−valence correlation, with a 5Z shift of −0.0123 to −0.0127 Å. This geometric shift brings the aCV5Z-DK and awCV5Z-DK bond lengths closer to the experimental value, within 0.003 Å. The frozen-core Br_2 ω_e values are in closer agreement to the experimental value, while core−valence correlation effects raise the harmonic frequencies by 3.3−3.4 cm^{-1}, a phenomenon that seems to be typical in the later third-row homonuclear diatomics. Removal of atomic spin−orbit splitting will raise the experimental D_0 value (45.44 kcal mol^{-1})[106] by 7.0 kcal mol^{-1}. Our ZPE-corrected 5Z D_0 value is 51.1−51.2 kcal mol^{-1} and similar to the previous results of Feller et al.[53] Core−valence correlation has a small effect on the overall dissociation energy (only 0.2−0.3 kcal mol^{-1} at the 5Z level). Performing CBS extrapolations on the aug-cc-p(w)CV*n*Z-DK energies and adding molecular second-order spin−orbit effects should bring our result to within a few tenths of a kcal/mol of the experimental D_0. As with the closed-shell As_2 molecule, the D_0 value for Br_2 obtained by Widmark and co-authors is almost 4 kcal mol^{-1} lower than that of experiment.[82]

F. Kr_2. Spectroscopic properties of the weakly bound $X^1\Sigma_g^+$ krypton dimer have been measured experimentally by LaRocque and co-workers using fluorescence excitation techniques[108] and previously by Tanaka and co-workers via vacuum ultraviolet absorption spectroscopy.[109] Recent coupled cluster studies have provided a robust theoretical comparison.[110,111] Surprisingly, the effect of core−valence correlation on the Kr_2 bond length is significant, with a shift of −0.0229 Å calculated with the awCV5Z-DK basis set. Core−valence correlation effects improve the bond length tremendously, bringing the quintuple-ζ r_e values to within 0.008 Å of the experimental value. These

bond lengths are a few hundredths of an angstrom better than those of previous frozen-core coupled cluster studies on Kr_2.[110,111] Core−valence correlation has a negligible effect on the dissociation energy and harmonic frequency of Kr_2, with quintuple-ζ shifts less than 0.2 kcal/mol and 2 cm^{-1}, respectively. In accord with previous theoretical studies, the CCSD(T) D_e and ω_e values are quite accurate with large CV basis sets. It should be noted that the small linear dependencies that exist in the aCVQZ and aCV5Z basis sets, mainly due to the tight s functions, led to small numerical instabilities in the Kr_2 potential curves that affected the accuracy of the vibrational anharmonicity constants. This was overcome by taking a similar approach with the s-type functions as that described above with the p-type functions in the CV 5Z sets. Hence, only the first three HF s contractions were retained, and the most diffuse seven (quadruple-ζ) and eight (quintuple-ζ) functions were uncontracted.

Conclusions

The correlation consistent basis sets for the third-row, main group atoms Ga through Kr are extended to properly describe core−core and core−valence electron correlation. Atomic and molecular correlation energies as well as spectroscopic properties appear to converge monotonically to the CBS limit. When a proper treatment of core−valence correlation is added to accurate frozen-core calculations already including scalar relativistic effects, molecular results are shown to achieve a very high level of accuracy. Inclusion of core−core and core−valence electron correlation results in consistent effects on spectroscopic properties, shortening bond lengths and raising harmonic vibrational frequency values while generally increasing dissociation energies. As observed previously for the first- and second-row elements, the cc-pwCV*n*Z family of basis sets yields a faster convergence of the CV correlation effects on these spectroscopic constants compared to that of the cc-pCVnZ ones.

Calculations that account for core−valence effects by using correlation consistent basis sets without additional tight functions to describe the core region of the electron density are shown to be very unreliable, in accord with previous first- and second-row studies. Calculations where only the 3d core is added to the correlation space gives very similar results compared to those of the full 3s3p3d correlation space. However, at least for the Ga_2 molecule, the effects of including the 3s and 3p electrons are significant enough to be required for high-accuracy work.

Acknowledgment. CASCaM is supported by a grant from the United States Department of Education. This research is partially supported by a National Science Foundation CAREER Award CHE-0239555 (to A.K.W.). Computations employed the UNT computational chemistry resource, whose purchase was supported by a National Science Foundation CRIF grant (CHE-0342824). Dr. Scott Yockel and Brian Prascher are thanked for helpful discussions and comments.

Supporting Information Available: The exponents of optimized core−valence-correlating functions for the cc-pCV*n*Z and cc-pwCV*n*Z (n = D, T, Q, 5) basis sets for the elements Ga through Kr are provided in the Supporting Information. This material is available free of charge via the Internet at http://pubs.acs.org.

References and Notes

(1) Dunning, T. H., Jr. *J. Chem. Phys.* **1989**, *90*, 1007.
(2) Feller, D. *J. Chem. Phys.* **1992**, *96*, 6104.
(3) Martin, J. M. L. *Chem. Phys. Lett.* **1996**, *259*, 669.
(4) Wilson, A. K.; Dunning, T. H., Jr. *J. Chem. Phys.* **1997**, *106*, 8718.
(5) Feller, D.; Peterson, K. A.; Crawford, T. D. *J. Chem. Phys.* **2006**, *124*, 054107.
(6) Woon, D. E.; Dunning, T. H., Jr. *J. Chem. Phys.* **1993**, *99*, 1914.
(7) Dunning, T. H., Jr.; Peterson, K. A.; Wilson, A. K. *J. Chem. Phys.* **2001**, *114*, 9244.
(8) Wilson, A. K.; Woon, D. E.; Peterson, K. A.; Dunning, T. H., Jr. *J. Chem. Phys.* **1999**, *110*, 7667.
(9) Wilson, A. K.; Woon, D. E.; Peterson, K. A.; Dunning, T. H., Jr. *Abstr. Pap.—Am. Chem. Soc.* **1997**, *213*, 60.
(10) Kendall, R. A.; Dunning, T. H., Jr.; Harrison, R. J. *J. Chem. Phys.* **1992**, *96*, 6796.
(11) Woon, D. E.; Dunning, T. H., Jr. *J. Chem. Phys.* **1994**, *100*, 2975.
(12) Hess, B. A. *Phys. Rev. A* **1986**, *33*, 3742.
(13) Hess, B. A. *Phys. Rev. A* **1985**, *32*, 756.
(14) Douglas, M.; Kroll, N. M. *Ann. Phys.* **1974**, *82*, 89.
(15) de Jong, W. A.; Harrison, R. J.; Dixon, D. A. *J. Chem. Phys.* **2001**, *114*, 48.
(16) DeYonker, N. J.; Cundari, T. R.; Wilson, A. K. *J. Chem. Phys.* **2006**, *124*, 114104.
(17) Peterson, K. A. *J. Chem. Phys.* **2003**, *119*, 11099.
(18) Peterson, K. A.; Figgen, D.; Goll, E.; Stoll, H.; Dolg, M. *J. Chem. Phys.* **2003**, *119*, 11113.
(19) Peterson, K. A.; Puzzarini, C. *Theor. Chem. Acc.* **2005**, *114*, 283.
(20) Peterson, K. A.; Figgen, D.; Dolg, M.; Stoll, H. *J. Chem. Phys.* **2007**, *126*.
(21) Balabanov, N. B.; Peterson, K. A. *J. Chem. Phys.* **2005**, *123*, 064107.
(22) Woon, D. E.; Dunning, T. H., Jr. *J. Chem. Phys.* **1995**, *103*, 4572.
(23) Peterson, K. A.; Dunning, T. H., Jr. *J. Chem. Phys.* **2002**, *117*, 10548.
(24) Curtiss, L. A.; Raghavachari, K. *Theor. Chem. Acc.* **2002**, *108*, 61.
(25) Curtiss, L. A.; Raghavachari, K.; Redfern, P. C.; Pople, J. A. *J. Chem. Phys.* **2000**, *112*, 7374.
(26) Curtiss, L. A.; Raghavachari, K.; Redfern, P. C.; Rassolov, V.; Pople, J. A. *J. Chem. Phys.* **1998**, *109*, 7764.
(27) Curtiss, L. A.; Redfern, P. C.; Raghavachari, K.; Pople, J. A. *J. Chem. Phys.* **2001**, *114*, 108.
(28) Curtiss, L. A.; Redfern, P. C.; Raghavachari, K. *J. Chem. Phys.* **2005**, *123*, 124017.
(29) DeYonker, N. J.; Grimes, T.; Yockel, S.; Dinescu, A.; Mintz, B.; Cundari, T. R.; Wilson, A. K. *J. Chem. Phys.* **2006**, *125*, 104111.
(30) Ho, D. S.; DeYonker, N. J.; Wilson, A. K.; Cundari, T. R. *J. Phys. Chem. A* **2006**, *110*, 9767.
(31) DeYonker, N. J.; Peterson, K. A.; Steyl, G.; Wilson, A. K.; Cundari, T. R. *J. Phys. Chem. A* **2007**, doi: 10.1021/jp0715023.
(32) Petersson, G. A.; Frisch, M. J. *J. Phys. Chem. A* **2000**, *104*, 2183.
(33) Montgomery, J. A.; Frisch, M. J.; Ochterski, J. W.; Petersson, G. A. *J. Chem. Phys.* **1999**, *110*, 2822.
(34) Petersson, G. A. *Abstr. Pap.—Am. Chem. Soc.* **1996**, *212*, 175.
(35) Ochterski, J. W.; Petersson, G. A.; Montgomery, J. A. *J. Chem. Phys.* **1996**, *104*, 2598.
(36) East, A. L. L.; Allen, W. D. *J. Chem. Phys.* **1993**, *99*, 4638.
(37) Kenny, J. P.; Allen, W. D.; Schaefer, H. F. *J. Chem. Phys.* **2003**, *118*, 7353.
(38) Gonzales, J. M.; Pak, C.; Cox, R. S.; Allen, W. D.; Schaefer, H. F.; Császár, A. G.; Tarczay, G. *Chem.—Eur. J.* **2003**, *9*, 2173.
(39) Császár, A. G.; Allen, W. D.; Schaefer, H. F. *J. Chem. Phys.* **1998**, *108*, 9751.
(40) Császár, A. G.; Allen, W. D.; Yamaguchi, Y.; Schaefer, H. F. Ab Initio Determination of Accurate Ground Electronic State Potential Energy Hypersurfaces for Small Molecules. In *Computational Molecular Spectroscopy*; Jensen, P., Bunker, P. R., Eds.; John Wiley & Sons, Ltd.: New York, 2000; p 15.
(41) Császár, A. G.; Szalay, P. G.; Leininger, M. L. *Mol. Phys.* **2002**, *100*, 3879.
(42) Császár, A. G.; Leininger, M. L.; Burcat, A. *J. Phys. Chem. A* **2003**, *107*, 2061.
(43) Császár, A. G.; Leininger, M. L.; Szalay, V. *J. Chem. Phys.* **2003**, *118*, 10631.
(44) Parthiban, S.; Martin, J. M. L. *J. Chem. Phys.* **2001**, *114*, 6014.
(45) Martin, J. M. L.; de Oliveira, G. *J. Chem. Phys.* **1999**, *111*, 1843.
(46) Boese, A. D.; Oren, M.; Atasoylu, O.; Martin, J. M. L.; Kallay, M.; Gauss, J. *J. Chem. Phys.* **2004**, *120*, 4129.
(47) Karton, A.; Rabinovich, E.; Martin, J. M. L.; Ruscic, B. *J. Chem. Phys.* **2006**, *125*.
(48) Szalay, P. G.; Tajti, A.; Stanton, J. F. *Mol. Phys.* **2005**, *103*, 2159.
(49) Tajti, A.; Szalay, P. G.; Császár, A. G.; Kallay, M.; Gauss, J.; Valeev, E. F.; Flowers, B. A.; Vazquez, J.; Stanton, J. F. *J. Chem. Phys.* **2004**, *121*, 11599.
(50) Bomble, Y. J.; Vazquez, J.; Kallay, M.; Michauk, C.; Szalay, P. G.; Császár, A. G.; Gauss, J.; Stanton, J. F. *J. Chem. Phys.* **2006**, *125*.

(51) Feller, D.; Dixon, D. A. *J. Phys. Chem. A* **2003**, *107*, 9641.
(52) Feller, D.; Dixon, D. A.; Francisco, J. S. *J. Phys. Chem. A* **2003**, *107*, 1604.
(53) Feller, D.; Peterson, K. A.; de Jong, W. A.; Dixon, D. A. *J. Chem. Phys.* **2003**, *118*, 3510.
(54) Dixon, D. A.; Feller, D.; Francisco, J. S. *J. Phys. Chem. A* **2003**, *107*, 186.
(55) Dixon, D. A.; Feller, D.; Peterson, K. A. *J. Chem. Phys.* **2001**, *115*, 2576.
(56) Feller, D.; Dixon, D. A. *J. Phys. Chem. A* **2000**, *104*, 3048.
(57) Dixon, D. A.; Feller, D.; Sandrone, G. *J. Phys. Chem. A* **1999**, *103*, 4744.
(58) Feller, D.; Dixon, D. A. *J. Phys. Chem. A* **1999**, *103*, 6413.
(59) Dixon, D. A.; Peterson, K. A.; Francisco, J. S. *J. Phys. Chem. A* **2000**, *104*, 6227.
(60) Dixon, D. A.; de Jong, W. A.; Peterson, K. A.; Francisco, J. S. *J. Phys. Chem. A* **2002**, *106*, 4725.
(61) Pollack, L.; Windus, T. L.; de Jong, W. A.; Dixon, D. A. *J. Phys. Chem. A* **2005**, *109*, 6934.
(62) Curtiss, L. A.; Redfern, P. C.; Rassolov, V.; Kedziora, G.; Pople, J. A. *J. Chem. Phys.* **2001**, *114*, 9287.
(63) Blaudeau, J. P.; Curtiss, L. A. *Int. J. Quantum Chem.* **1997**, *61*, 943.
(64) Deutsch, P. W.; Curtiss, L. A.; Blaudeau, J. P. *Chem. Phys. Lett.* **1997**, *270*, 413.
(65) Hennum, A. C.; Halkier, A.; Klopper, W. *J. Mol. Struct.* **2001**, *599*, 153.
(66) de Lara-Castells, M. P.; Krems, R. V.; Buchachenko, A. A.; Delgado-Barrio, G.; Villarreal, P. *J. Chem. Phys.* **2001**, *115*, 10438.
(67) Sari, L.; Peterson, K. A.; Yamaguchi, Y.; Schaefer, H. F. *J. Chem. Phys.* **2002**, *117*, 10008.
(68) Koizumi, H.; Davalos, J. Z.; Baer, T. *Chem. Phys.* **2006**, *324*, 385.
(69) Press, W. H.; Teulosky, S. A.; Vetterling, W. T.; Flannery, B. P. *Numerical Recipies in FORTRAN: The Art of Scientific Computing*, 2nd ed.; Cambridge University Press: Cambridge, U.K., 1992.
(70) Raghavachari, K.; Trucks, G. W.; Pople, J. A.; Head-Gordon, M. *Chem. Phys. Lett.* **1989**, *157*, 479.
(71) Rittby, M.; Bartlett, R. J. *J. Phys. Chem.* **1988**, *92*, 3033.
(72) Knowles, P. J.; Hampel, C.; Werner, H.-J. *J. Chem. Phys.* **1993**, *99*, 5219.
(73) Bauschlicher, C. W., Jr. *J. Phys. Chem. A* **1998**, *102*, 10424.
(74) Martin, J. M. L.; Sundermann, A. *J. Chem. Phys.* **2001**, *114*, 3408.
(75) See Supporting Information.
(76) Huber, K. P.; Herzberg, G. *Molecular Spectra and Molecular Structure IV. Constants of Diatomic Molecules*; Van Nostrand Reinhold: New York, 1979.
(77) Ginter, D. S.; Ginter, M. L.; Innes, K. K. *J. Phys. Chem.* **1965**, *69*, 2480.
(78) Froben, F. W.; Schulze, W.; Kloss, U. *Chem. Phys. Lett.* **1983**, *99*, 500.
(79) Balasubramanian, K. *J. Phys. Chem.* **1986**, *90*, 6786.
(80) Shim, I.; Mandix, K.; Gingerich, K. A. *J. Phys. Chem.* **1991**, *95*, 5435.
(81) Ghosh, T. K.; Tanaka, K.; Mochizuki, Y. *J. Mol. Struct.: THEOCHEM* **1998**, *451*, 61.
(82) Roos, B. O.; Lindh, R.; Malmqvist, P. A.; Veryazov, V.; Widmark, P. O. *J. Phys. Chem. A* **2004**, *108*, 2851.
(83) Balducci, G.; Gigli, G.; Meloni, G. *J. Chem. Phys.* **1998**, *109*, 4384.
(84) Tan, X.; Dagdigian, P. J. *J. Phys. Chem. A* **2003**, *107*, 2642.
(85) Greetham, G. M.; Ellis, A. M. *J. Mol. Spectrosc.* **2003**, *222*, 273.
(86) Himmel, H.-J.; Gaertner, B. *Chem.−Eur. J.* **2004**, *10*, 5936.
(87) Das, K. K. *J. Phys. B: At. Mol. Opt. Phys.* **1997**, *30*, 803.
(88) Moore, C. E. *Atomic Energy Levels*; U.S. Department of Commerce: Washington, DC, 1971; Vol. 2.
(89) Pacchioni, G. *Mol. Phys.* **1983**, *49*, 727.
(90) Northrup, J. E.; Cohen, M. L. *Chem. Phys. Lett.* **1983**, *102*, 440.
(91) Kingcade, J. E.; Nagarathna-Naik, H. M.; Shim, I.; Gingerich, K. A. *J. Phys. Chem.* **1986**, *90*, 2830.
(92) Shim, I.; Baba, M. S.; Gingerich, K. A. *Chem. Phys.* **2002**, *277*, 9.
(93) Hostutler, D. A.; Li, H.; Clouthier, D. J.; Wannous, G. *J. Chem. Phys.* **2002**, *116*, 4135.
(94) Clouthier, C.; Grein, F.; Bruna, P. J. *Mol. Phys.* **2005**, *103*, 3253.
(95) Li, S.; Zee, R. J. V.; Weltner, W. J. *J. Chem. Phys.* **1994**, *100*, 7079.
(96) Wang, L.-S.; Lee, Y. T.; Shirley, D. A.; Balasubramanian, K.; Feng, P. *J. Chem. Phys.* **1990**, *93*, 6310.
(97) Shen, M.; Schaefer, H. F. *J. Chem. Phys.* **1994**, *101*, 2261.
(98) Yockel, S.; Mintz, B.; Wilson, A. K. *J. Chem. Phys.* **2004**, *121*, 60.
(99) Yockel, S.; Wilson, A. K. *J. Chem. Phys.* **2005**, *122*, 174310.
(100) Balasubramanian, K. *J. Phys. Chem.* **1987**, *91*, 5166.
(101) Kohara, S.; Goldbach, A.; Koura, N.; Saboungi, M. L.; Curtiss, L. A. *Chem. Phys. Lett.* **1998**, *287*, 282.
(102) Pan, B. C.; Han, J. G.; Yang, J. L.; Yang, S. H. *Phys. Rev. B* **2000**, *62*, 17026.
(103) Prosser, S. J.; Barrow, R. F.; Effantin, C.; d'Incan, J.; Vergès, J. *J. Phys. B: At. Mol. Opt. Phys.* **1982**, *15*, 4151.
(104) Fink, E. H.; Setzer, K. D.; Ramsay, D. A.; Zhu, Q.-S. *Can. J. Phys.* **1994**, *72*, 919.
(105) Setzer, K. D.; Dorn, A.; Lorenz, M.; Fink, E. H. *J. Mol. Spectrosc.* **2003**, *221*, 13.
(106) Focsa, C.; Li, H.; Bernath, P. F. *J. Mol. Spectrosc.* **2000**, *200*, 104.
(107) Shepler, B. C.; Peterson, K. A. *J. Phys. Chem. A* **2006**, *110*, 12321.
(108) LaRocque, P. E.; Lipson, R. H.; Herman, P. R.; Stoicheff, B. P. *J. Chem. Phys.* **1986**, *84*, 6627.
(109) Tanaka, Y.; Yoshino, K.; Freeman, D. E. *J. Chem. Phys.* **1973**, *59*, 5160.
(110) Slavíček, P.; Kalus, R.; Paška, P.; Odvárková, I.; Hobza, P.; Malijevský, A. *J. Chem. Phys.* **2003**, *119*, 2102.
(111) Haley, T. P.; Cybulski, S. M. *J. Chem. Phys.* **2003**, *119*, 5487.
(112) Binning, R. C., Jr.; Curtiss, L. A. *J. Comput. Chem.* **1990**, *11*, 1206.